Global monitoring of large reservoir storage from satellite remote sensing

Huilin Gao,[1,2] Charon Birkett,[3] and Dennis P. Lettenmaier[1]

Received 29 February 2012; revised 5 July 2012; accepted 9 July 2012; published 5 September 2012.

[1] We studied 34 global reservoirs for which good quality surface elevation data could be obtained from a combination of five satellite altimeters for the period from 1992 to 2010. For each of these reservoirs, we used an unsupervised classification approach using the Moderate Resolution Imaging Spectroradiometer (MODIS) 16-day 250 m vegetation product to estimate the surface water areas over the MODIS period of record (2000 to 2010). We then derived elevation-area relationships for each of the reservoirs by combining the MODIS-based estimates with satellite altimeter-based estimates of reservoir water elevations. Through a combination of direct observations of elevation and surface area along with documented reservoir configurations at capacity, we estimated storage time histories for each reservoir from 1992 to 2010. We evaluated these satellite-based data products in comparison with gauge observations for the five largest reservoirs in the United States (Lakes Mead, Powell, Sakakawea, Oahe, and Fort Peck Reservoir). The storage estimates were highly correlated with observations (R = 0.92 to 0.99), with values for the normalized root mean square error (NRMSE) ranging from 3% to 15%. The storage mean absolute error (expressed as a percentage of reservoir capacity) for the reservoirs in this study was 4%. The multidecadal reconstructed reservoir storage variations are in accordance with known droughts and high flow periods on each of the five continents represented in the data set.

Citation: Gao, H., C. Birkett, and D. P. Lettenmaier (2012), Global monitoring of large reservoir storage from satellite remote sensing, *Water Resour. Res.*, *48*, W09504, doi:10.1029/2012WR012063.

1. Introduction

[2] Reservoirs are key tools for the management of water resources. They provide a means for reducing the effects of interseasonal and interannual streamflow fluctuations and hence facilitating water supply, flood control, hydroelectric power generation, recreation, and other water uses. *Nilsson et al.* [2005] found that over half of the world's large river systems are currently impacted by dams. Since the era of large dam construction began about a century ago, the sequestration of water in reservoirs may have reduced sea level rise by as much as 30 mm, with a rate of more than 0.5 mm y^{-1} near the middle of twentieth century [*Chao et al.*, 2008; *Lettenmaier and Milly*, 2009]. A total of more than 33,000 large dams are included in the *World Register of Dams*, with a total storage capacity of about 8300 km^3 in 2000 [*Chao et al.*, 2008; *International Commission on Large Dams*, 2007]. In contrast to the comprehensive documentation of the dams and their configurations, consistent observations of reservoir storage are limited mostly to developed countries, and even there the records are often difficult to access. This unbalanced spatial distribution of observational data makes it challenging to assess the effects of human alterations to the land hydrologic cycle, which are not well represented in current earth system models.

[3] Modeling approaches have been used to simulate reservoir storage in lieu of direct observations. On continental and global scales, most studies have focused on reservoir impacts on downstream river discharge [*Döll et al.*, 2009; *Haddeland et al.*, 2006; *Hanasaki et al.*, 2006]. Unfortunately, the calibrations and validations of these models are mostly limited to North America, where gauge observations are relative easy to access. For the rest of the world, especially the less populated and underdeveloped regions, there are large, unresolved disparities among these modeling results. For example, *Biemans et al.* [2011] found that the estimates for irrigation water demand around the year 2000 ranged from 1900 km^3 y^{-1} to 3800 km^3 y^{-1} [*Döll and Siebert*, 2002; *Rost et al.*, 2008, and references therein; *Vörösmarty et al.*, 2005; *Wisser et al.*, 2008]. Consequently, results from global reservoir simulations are questionable in terms of their utility for quantitative analysis and decision making in those regions where there are no direct observations of reservoir storage.

[4] Beginning about 2 decades ago, satellite remote sensing began to show promise for estimating water storage in large reservoirs and lakes. This breakthrough is attributable to the

[1]Department of Civil and Environmental Engineering, University of Washington, Seattle, Washington, USA.
[2]Now at Zachry Department of Civil Engineering, Texas A&M University, College Station, Texas, USA.
[3]ESSIC, University of Maryland, College Park, Maryland, USA.

Corresponding author: D. P. Lettenmaier, Department of Civil and Environmental Engineering, University of Washington, Seattle, WA 98195, USA. (dennisl@u.washington.edu)

advent of satellite radar altimetry [*Berry et al.*, 2005; *Birkett*, 1994, 1995], the primary purpose of which is to obtain estimates of ocean surface topography (notwithstanding that some satellite altimeters have secondary purposes such as ice sheet and sea ice mapping). Despite issues with spatial resolution, related both to the relatively long along-track path length required to obtain accurate vertical measurements (typically 10 km or so), and coarse across-track spacing (order of hundreds of kilometers), satellite altimetry is considered the best method for measuring water elevation variations from space [*Alsdorf et al.*, 2007; *Tang et al.*, 2009]. The most commonly used spaceborne radar altimeters are GEOSAT (1986–1988), Topex/Poseidon (T/P) (1992–2002), ERS-1 (1991–1996), ERS-2 (1995–2003), GFO (2000–2008), ENVISAT (post-2002), JASON-1 (post 2002), and JASON-2 (post 2008). Typical radar altimetry vertical precision is several tens of centimeters. For very large lakes with no interference of the radar echo from land (e.g., the Great Lakes) the satellite measurement error can be as small as a few centimeters. Smaller lakes, large lakes with interference of the radar echo from land, or lakes with low surface roughness (calm conditions) will all have larger errors. Although surface water elevations from altimetry are available for both lakes and reservoirs [*Alsdorf et al.*, 2001; *Berry et al.*, 2005; *Birkett*, 1994; *Crétaux et al.*, 2011], most applications to date have focused on lakes [*Birkett*, 2000; *Aladin et al.*, 2005; *Crétaux et al.*, 2005; *Mercier et al.*, 2002; *Xu et al.*, 2006].

[5] To estimate water storage (and storage variation) in lakes and reservoirs, measurements of both surface water area and bathymetry are needed. Surface water extent can be measured from optical sensors, such as Landsat and the Moderate-Resolution Imaging Spectroradiometer (MODIS), as well as from Synthetic Aperture Radar (SAR) sensors, such as RADARSAT, JERS-1, and ERS. The primary advantage of Landsat is its high resolution (30 m), but it has low repeat frequency and is susceptible to cloud cover contamination. For sensors with daily coverage, like MODIS, the frequency of observations is obviously an advantage, but the resolution is relatively coarse (250 m to 500 m at the visible and near infrared bands). Although a static global water mask has been produced using MODIS and Shuttle Radar Topography Mission (SRTM) observations at 250 m resolution [*Carroll et al.*, 2009], dynamic water classification estimates have been limited to case studies [e.g., *Islam et al.*, 2010; *Wang et al.*, 2008]. A common practice for MODIS-based water classification is to place some thresholds on selected vegetation indexes for decision making, but the thresholds are often empirical and vary case by case. Multitemporal interferometric SAR imagery can be used to delineate surface water. This approach is based on the assumption that the repeat-pass coherence over water is much smaller (because the scattering characteristics of water surfaces continually change with waves) than the coherence over the surrounding land (the land surface characteristics remain static in the interferometric pairs which are 1 day apart) [*Smith and Alsdorf*, 1998]. However, such a condition is not met in most circumstances by SARs with more than a few day repeat cycles since snow, rain, and wind between acquisitions can alter dielectric properties of the surrounding area and result in poor coherence everywhere in the imagery [*Alsdorf et al.*, 2007].

[6] Notwithstanding the possibility of monitoring both elevation and surface area of reservoirs and lakes from space, most satellite-based methods combine them with in situ observations [*Sawunyama et al.*, 2006; *Xu et al.*, 2006]. This is a major obstacle for studies in data sparse regions. *Crétaux et al.* [2011] were the first to monitor storage variations of lakes using satellite data exclusively. For estimation of lake surface area, they used different sources of satellite imagery, such as Landsat, MODIS, ASAR (from the Envisat satellite), and others. Perhaps because of the large diversity of sensor frequencies, spatial resolutions, and repeat cycles, detailed description of the water classification algorithms utilized for the lake surface area estimation and the errors in the estimates were not provided, nor were the surface area and storage variations compared with surface observations.

[7] This study has two objectives: (1) to create time histories of reservoir storage for selected large reservoirs globally using only remote sensing observations, with reservoir surface area as a by-product; and (2) to analyze the errors in the products using in situ observations where available.

2. Data and Methodology

[8] We describe in this section the remote sensing data sources and the methods we use to estimate reservoir water levels, surface areas, and storages.

2.1. Reservoir Water Level From Radar Altimetry

[9] Satellite radar altimetry was designed primarily to measure water levels over the open ocean. Although many factors (such as the narrow swath, low spatial resolution, small footprint size, and complex terrain around some inland water bodies) eliminate the possibility for monitoring most small water bodies with current satellite sensors, altimetry has demonstrated great potential for hydrological studies for some large inland water bodies globally. Surface elevation data sets for large lakes and reservoirs globally are available from the U.S. Department of Agriculture's (USDA) Global Reservoir and Lake Elevation Database (http://www.pecad.fas.usda.gov/cropexplorer/global_reservoir/); the French Space Agency Centre National d'Etudes Spatiales' (CNES) Hydrology by Altimetry (http://www.legos.obs-mip.fr/soa/hydrologie/hydroweb/); and the European Space Agency's (ESA) River and Lake data set (http://tethys.eaprs.cse.dmu.ac.uk/RiverLake/shared/main). At the time of this research (2010), the USDA and CNES databases provided 20 and 36 reservoir data products, respectively. The ESA data set primarily focuses on rivers and lakes (with a few reservoirs which are also included in the other two data sets).

[10] In addition to the reservoirs included in these existing data sets, we retrieved water elevation levels for another 20 reservoirs from Topex/Poseidon (T/P) for the period 1992 to 2002 (hereafter referred to as University of Washington (UW)). These reservoirs were identified by overlaying the T/P orbits onto the reservoir maps from the Global Lakes and Wetland Database (GLWD) [*Lehner and Döll*, 2004]. The data processing procedures were similar to those used to produce the USDA data product, which closely follow methods developed by the NASA Ocean Altimeter Pathfinder Project [*Chelton et al.*, 1988; *McKellip et al.*, 2004; *Ross*, 2006; *Birkett and Beckley*, 2010]. These three data sources (USDA, CNES, and UW) together provide 62 reservoir water level time series (after eliminating duplicates). From the combined data set, we chose 34 reservoirs as the

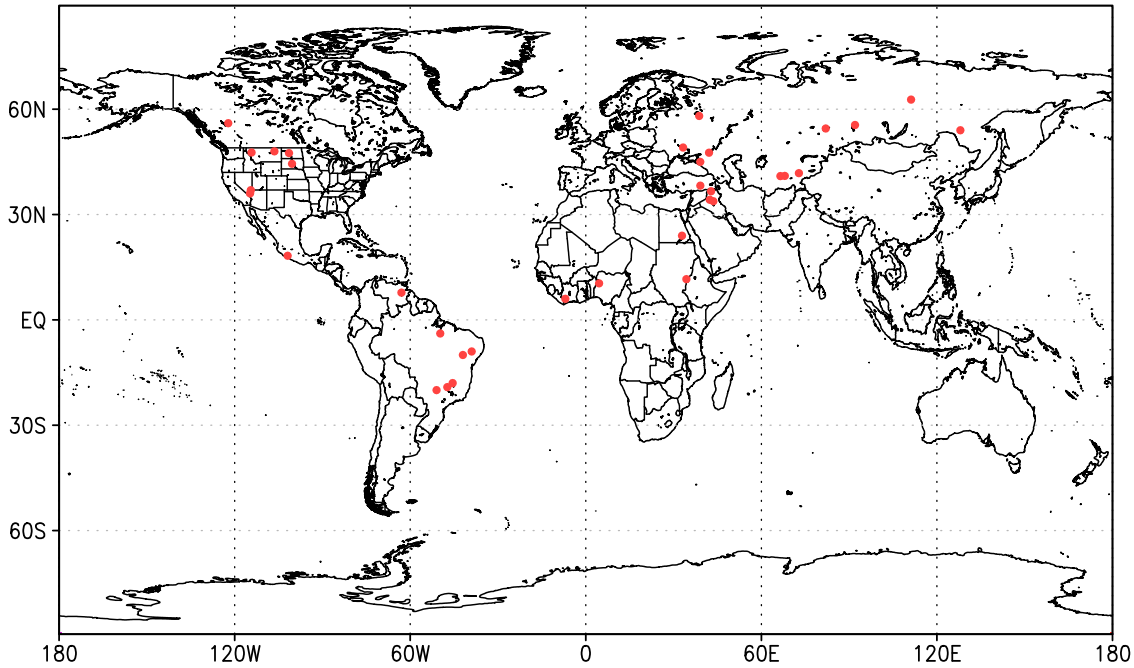

Figure 1. Locations of the study reservoirs.

focus for this study. The selection criteria were (1) the elevation time series had to cover at least 2 years after 2000 (when the MODIS data became available) so that a water level-surface area relationship could be established; (2) the remotely sensed reservoir levels had to show plausible seasonal variations based on a visual screening; (3) the reservoir water body had to be distinct from other nearby water bodies. Figure 1 shows the locations of the selected reservoirs.

2.2. Reservoir Surface Area From MODIS

[11] The MODIS/Terra 16-day L3 global vegetation indices at 250 m (MOD13Q1) from the NASA Land Processes Distributed Active Archive Center (http://lpdaac.usgs.gov/) were used to estimate reservoir surface area from 2000 to 2010. This choice was made on the basis of three factors: First, MODIS observed vegetation indices have been used previously to detect flood inundation [*Islam et al.*, 2010; *Ordoyne and Friedl*, 2008; *Yan et al.*, 2010]. Second, the 250 m resolution is the highest available from MODIS, which helps in representing the irregular shapes of many reservoirs. Third, the 16-day temporal resolution is close to the repeat cycle of most of the satellite altimeters and suffers much less from cloud contamination as compared to daily or 8-day products.

[12] A common practice for water classification using MODIS vegetation indices is to apply case-dependent thresholds in the decision trees [*Islam et al.*, 2010; *Xiao et al.*, 2006; *Yan et al.*, 2010]. Since the reservoirs in this study are located in different climate zones and are surrounded by different land cover types, we chose the nonparametric unsupervised K-means clustering classification approach [*Anderberg*, 1973; *MacQueen*, 1967]. To reduce the computational cost and increase the classification accuracy, the clustering was conducted only over each reservoir and a surrounding area. We use Fort Peck Reservoir (Montana, USA) as an example to illustrate the method used for area estimation.

[13] First, a uniform threshold of 0.1 was applied to the entire set of available normalized difference vegetation index (NDVI) images (250 images in total from 2000 to 2010) to produce an initial set of surface water estimates. Although the fixed 0.1 threshold is not precise, it does allow the shape of the reservoir polygons to be reasonably well estimated. The result of this process for each NDVI image was an image with three classes: water, land, and invalid. The invalid class represents the pixels that were defined as "unreliable" in the quality control (QC) file (e.g., covered by snow/ice or cloud). For each pixel within the domain for a given reservoir, the frequency (in terms of the percentage of the cell classified as water for the entire period) was calculated. A mask, within which the classifications were to be conducted, was then derived based on this frequency map. The masked area contains two types of pixels. The first type included all the cells that had a value larger than 10% (considered "water") in the frequency map (with a total area of 946 km^2 as compared to 996 km^2 at capacity). This process constituted a first pass. A second pass expanded the mask to include a ring area, which covered any "nonwater" area that fell within a 21 $\times$ 21 (cell) moving box centered on each water cell (from the first pass). With an area of 3327 km^2, the resulting mask was large enough that it included the reservoir regardless of its level. Figure 2 shows the delineated mask with the percentiles for the water class depicted.

[14] Next, a water classification was performed using the K-means clustering algorithm to extract the water area from the masked portion of each of the 250 NDVI images for the 2000–2010 period. The use of the mask serves two purposes: first, it reduces computational cost; second, it enhances classification accuracy by focusing on the reservoir and its surrounding area. Like many other unsupervised classification

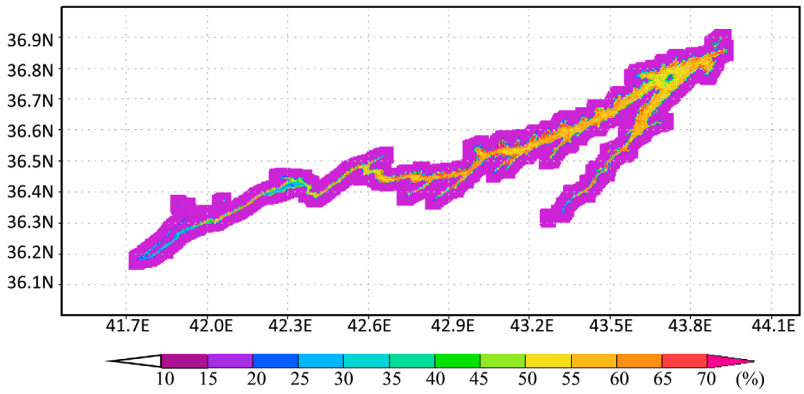

Figure 2. Delineated mask for Fort Peck Reservoir (with percentiles for water class).

approaches, K-means clustering is an iterative procedure. The objective is to minimize the variability within the cluster. The objective function (which is to be minimized) is the sum of squares of the distances (errors) between each pixel and its assigned cluster center [*Bobrowski and Bezdek*, 1991; *Selim and Ismail*, 1984]. Only the reliable NDVI grid cells (free of snow/ice/cloud contamination) within the masked area were used in the clustering. For each classified image, if the number of pixels with bad data quality (according the QC file) was more than 5% of the total number of pixels in the masked domain, we considered the result to be not usable. For those classified images with good data coverage, a majority filter (a simple post classification procedure which replaces cells in a raster based on the majority of their contiguous neighboring cells) was applied to the classified image to reduce the high spatial frequency noise ("salt and pepper" effect). Figure 3 shows two examples of the water classification results for Fort Peck reservoir, one for a high water elevation and the other for a low water elevation. Because the MOD13Q1 data use a sinusoidal projection, which is a pseudocylindrical equal-area map projection, each grid cell has a constant area of 62,500 m^2. For each classified image, reservoir surface area was estimated as the total area of the water cells. As an example, the time series of surface area for Fort Peck Reservoir is shown in Figure 4.

2.3. Estimation of Reservoir Storage

[15] The water elevations and surface areas (during any overlapping period(s) from 2000 to 2010) for each of the reservoirs were used to derive the elevation-area relationships. These elevation-area relationships were then used to estimate reservoir storage time series. Figure 5 shows results for Fort Peck Reservoir. A linear regression was used to approximate the relationship between surface elevation (h) and surface area (A), $A = f(h)$. For the period when MODIS data were unavailable (1992 to 2000), this relationship was applied to estimate the reservoir surface area from the water elevation. Similarly, during periods when altimetry data were unavailable during the MODIS era, the water elevation was estimated as an inverse function of the surface area

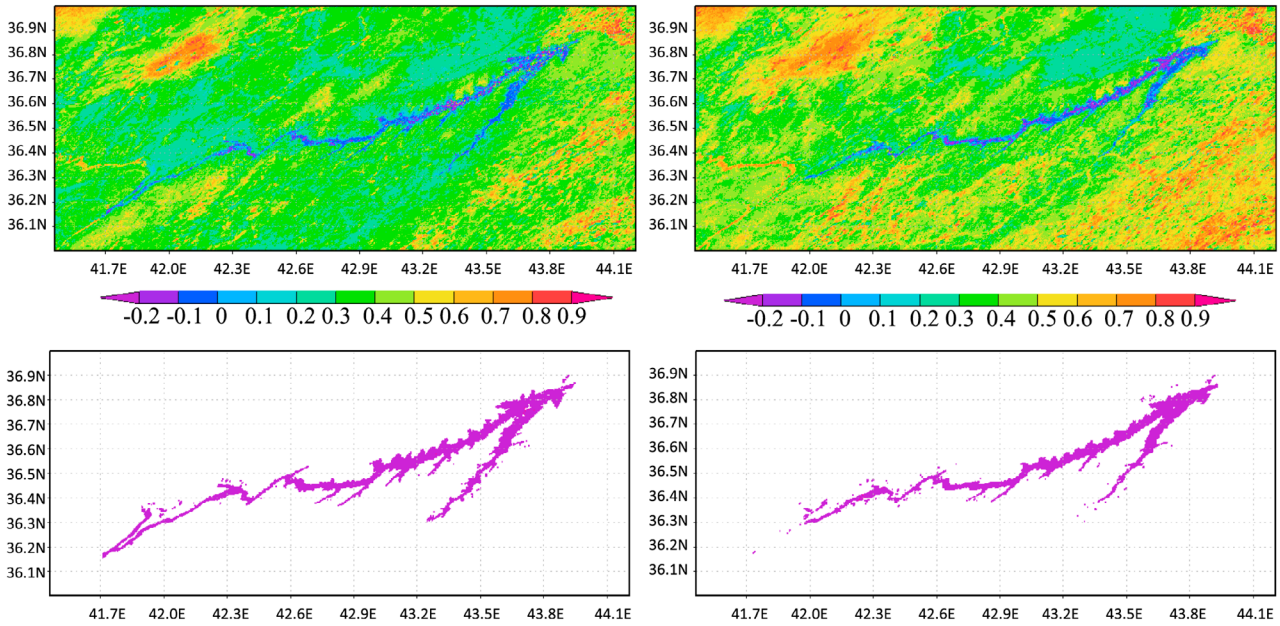

Figure 3. Examples of the water classification results for Fort Peck Reservoir, wet scenario (2000, day 177) and dry scenario (2005, day 177), showing (top) the NDVI images and (bottom) classification results.

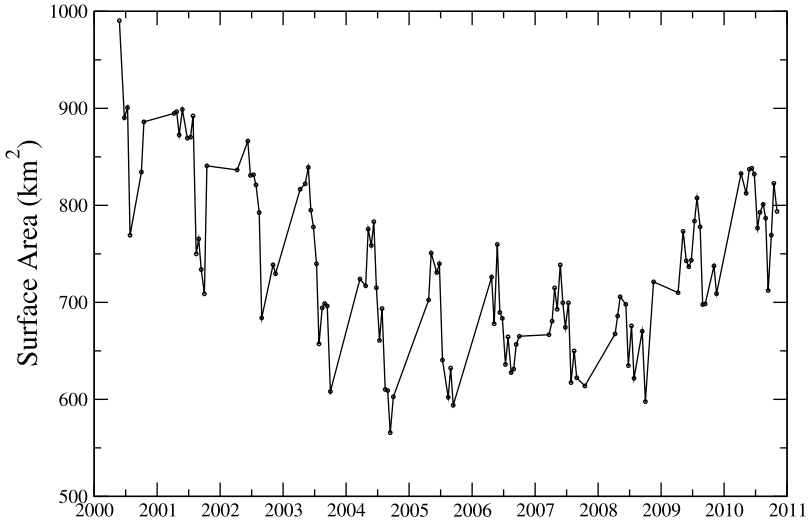

Figure 4. Time series of MODIS-estimated surface area for Fort Peck Reservoir.

function ($h = f^{-1}(A)$). Equation (1) was used to estimate reservoir storage, where V_c, A_c, and h_c represent storage, area, and water elevation at capacity, and V_o, A_o, and h_o are the observed storage, area, and water elevation, respectively. The values at capacity were taken mostly from the Global Reservoir and Dam (GRanD) database [*Lehner et al.*, 2011]. GRanD is based on multiple sources, including a variety of regional and national inventories and gazetteers, International Commission on Large Dam's World Register of Dams (www.icold-cigb.net), as well as a variety of publications, monographs, and maps. By substituting the elevation-area relationship into equation (1), the storage equation can be simplified into a single variable function, either as a function of water elevation from altimetry (referred as altimetry-estimated storage hereafter) or as a function of surface area from MODIS (referred as MODIS-estimated storage hereafter).

$$V_o = V_c - (A_c + A_o)(h_c - h_o)/2. \quad (1)$$

[16] Figure 6 shows the estimated storage time series for Fort Peck Reservoir. The MODIS-estimated storage shows a seasonal variation that is not consistent with the altimetry-estimated storage. This seasonality associated with the MODIS-estimated results is caused by subgrid spatial heterogeneity associated with pixels along the reservoir shores. Fort Peck Reservoir is a sinuous water body that is 216 km long at capacity. As a result, many of the MODIS 250 m × 250 m grid cells over the reservoir are border cells, partially covered by water and partially covered by land. For these pixels on the border, the effective NDVI is a weighted function of NDVI values for the water portion and the land portion. When seasonal variations of NDVI for the land portion are large, the effective NDVI for the mixed pixel will have a distinct seasonality even when the water portion has a fixed area. Consequently, the K-mean clustering (which minimizes the variability within the cluster) tends to overestimate the water area when the NDVI for the land is similar to that for the water. Likewise, the clustering underestimates the water area when the NDVI for the land is very different from that for the water. To remove the false seasonality, we used a moving average of the MODIS-estimated storages. The modified MODIS results agree quite well with the altimeter-estimated storages. For the overlapping period when both the altimeter-estimated and MODIS-estimated storage were available, the former was used in the final product. Because the storage estimates for 1992 to 2000 were exclusively based on altimetry, the altimeter-estimated storage was used for the post-2000 period (if available) to maximize the consistency within the time series. The only exception was when MODIS surface area data were available but the altimetry product was not, in which case the water elevation was inferred from MODIS to maximize the length of the storage record. We made this choice because the water elevations were generally more accurate than the surface areas (see sections 3 and 4). For a very few cases where the MODIS-estimated storage had larger seasonal variations than

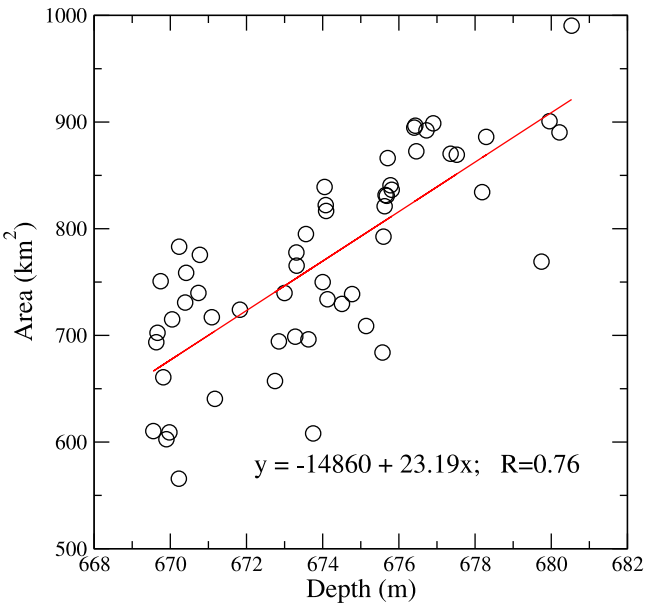

Figure 5. Water surface elevation surface area relationship for Fort Peck Reservoir.

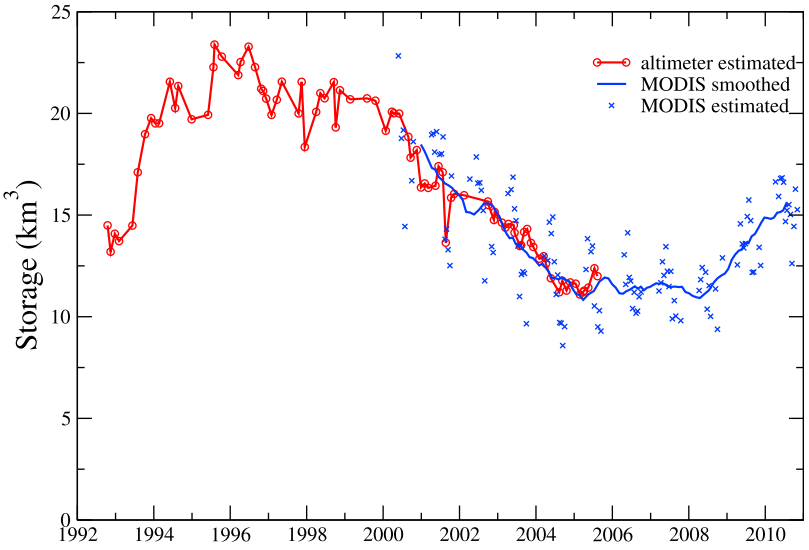

Figure 6. Time series of reservoir storage estimated from remote sensing for Fort Peck Reservoir.

the altimeter-estimated storage, the area based storage was smoothed using moving averages to make the results coherent.

3. Results

3.1. Evaluation for U.S. Reservoirs

[17] We performed error analyses on the satellite-based estimates using in situ observations for five large U.S. reservoirs (Lakes Mead, Powell, Sakakawea, Oahe, and Fort Peck Reservoir). Monthly observed reservoir elevations and storage were obtained from the U.S. Army Corps of Engineers and the U.S. Bureau of Reclamation. Elevation-volume relationships ($V = g(h)$) were derived for each reservoir from the observations. The reservoir area for each observed elevation was then estimated by taking the derivative of the volume, i.e., $A = \frac{dV}{dh} = g'(h)$. Figure 7 shows the evaluation results. The quantitative accuracy of reservoir elevation, area, and storage estimates were assessed using the correlation

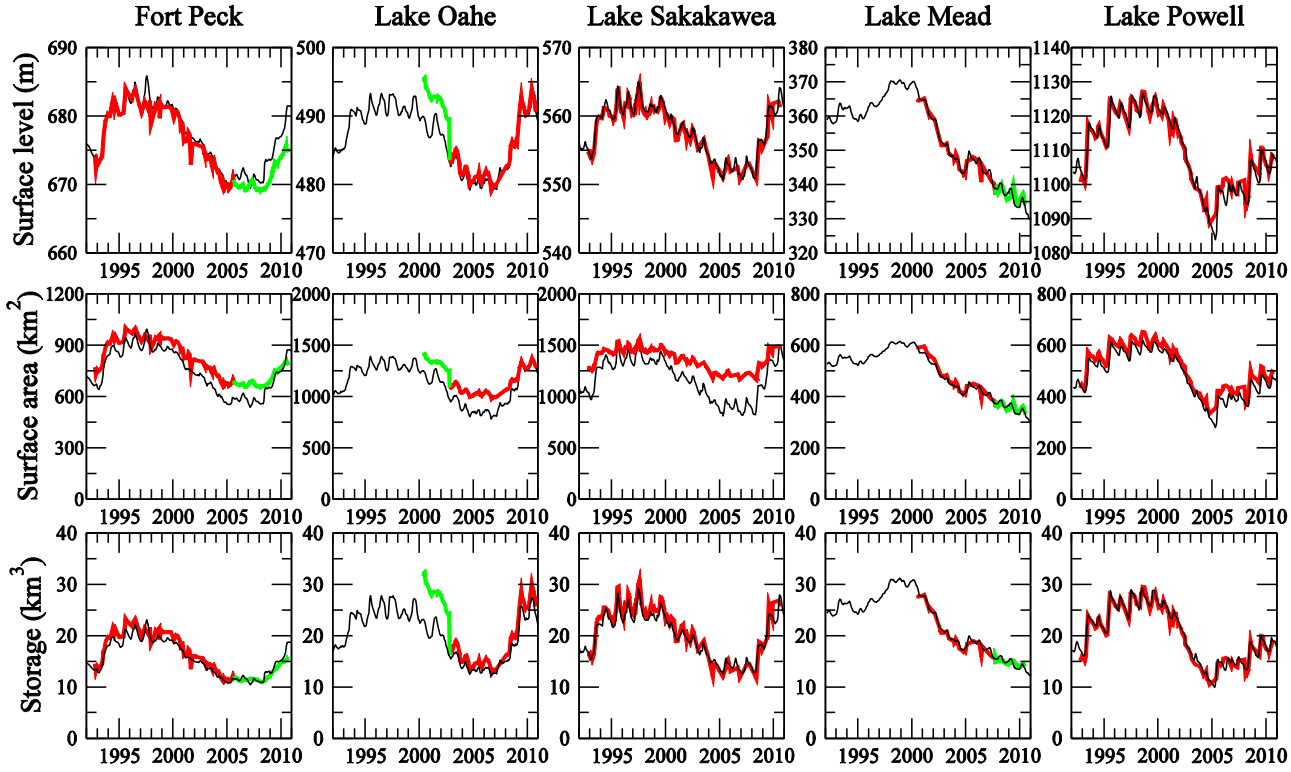

Figure 7. Evaluations of the water surface elevation, surface area, and storage from remote sensing compared with gauge observations for five U.S. reservoirs, with observations in black, altimetry-based estimates in red, and MODIS-based estimates in green.

Table 1. Summary of Comparisons Between Remotely Sensed Reservoir Data and Observations for Five U.S. Reservoirs[a]

		Fort Peck Reservoir	Lake Oahe	Lake Sakakawea	Lake Mead	Lake Powell
R	elevation	0.97	0.94	0.99	0.99	0.98
	area	0.97	0.94	0.99	0.99	0.98
	storage	0.97	0.92	0.99	0.99	0.99
Bias	elevation (m)	−1.08	1.57	0.28	−0.10	0.53
	area (km^2)	67	137	187	6	29
	storage (km^3)	0.63	2.87	0.53	−0.23	−0.21
NRMSE	elevation (%)	10	17	5	4	5
	area (%)	10	15	18	3	7
	storage (%)	8	15	7	3	3

[a]Reservoir data include elevations, areas, and storages.

coefficient (R), mean bias (defined as $bias = \overline{RS} - \overline{Obs}$, where $\overline{RS}$ and $\overline{Obs}$ are mean remote sensing and observation based estimates), and normalized root-mean square error ($NRMSE = \frac{\sqrt{\sum_{i=1}^{i=n} \frac{(RS_i - Obs_i)^2}{n}}}{\overline{Obs}} \times 100\%$, where RS_i and Obs_i denote remote sensing and observation based monthly estimates, and n is the number of pairs in the analysis). Table 1 summarizes the results of the error analysis. All of the satellite-estimated reservoir terms (water elevation, surface area, and storage) are highly correlated with observations (0.92 to 0.99), although these high correlations are attributable in part to common seasonal cycles in the estimates and observations. While the altimetry-estimated water elevation tends to have relatively small biases for all five reservoirs, the MODIS-estimated surface areas over the three Missouri Basin reservoirs tend to be biased upward especially during dry years. This likely occurs because these three reservoirs all have a combination of very long shorelines, large surface areas, and shallow depths. For the same storage change values, the variations of the Missouri Basin reservoirs areas are about triple those of the Colorado reservoirs. When the water elevations in these reservoirs decline, water retreats along the shoreline quickly. This shrinking in size leaves disconnected ponds, which are speckle-like in the classified images. When these dense speckles are further smoothed out using the majority filter, the water area is overestimated. Among the three Missouri reservoirs, Lake Oahe has the largest shoreline-to-sqrt(area) ratio (94, 48, and 37 for Oahe, Fort Peck, and Sakakawea respectively), which leads to some degree of overestimation even when the reservoir is relatively full. As a result, the elevation is biased high when it is inferred from the MODIS area. The error is further compounded in the storage results when only MODIS observations are available.

3.2. Global Data Set

[18] As described in section 2, after the elevation-surface area relationships for each of the 34 reservoirs were developed, they were used to estimate time series of reservoir storage. The reservoir storage results are shown in Figure 8 and the elevation-area relationships are summarized in Table 2. The total capacity of the 34 reservoirs is 1164 km^3, which represents about 15% of global reservoir capacity. For 16 of these reservoirs, the estimated storage is available for 19 years (1992–2010). The average record length for all reservoirs is 14.5 years. The correlation coefficient between the water elevation and surface area varies from 0.08 to 0.98, with an average value of 0.5. A high correlation usually indicates good quality for both data sets, while a low correlation can result from many conditions. These include errors from either the water elevation or surface area (or both) and/or the possibility that within the range of variation the bathymetry is independent of area (i.e., vertical walls). For consistency within the time series for each reservoir, the MODIS-estimated surface areas were used to maximize the record length (when altimetry water elevation was unavailable) only if the correlation coefficient between altimetry water elevation and MODIS surface area exceeded 0.5. We further discuss how these factors influence the correlations and ultimately the estimated storages in section 4. The elevation-area relationship is also used to derive two companion products: the inferred surface area and inferred water elevations where direct observations were unavailable.

[19] We selected a few reservoirs from each continent to explore the hydrological implications of this global data set. Lake Tharthar, the largest lake in Iraq, is the first example. Its primary purpose is irrigation. During our study period, there were two severe droughts in the Fertile Crescent, one from 1998 to 2001 and the other from 2008 to 2010 [*Trigo et al.*, 2010]. Both wheat and barley production dropped precipitously during these drought events. The remotely sensed reservoir storage for Lake Tharthar indicates that the lowest storage during these events is about 35% of the peak value in 1993. Lake Qadisiyah, a much smaller reservoir (also built for irrigation) close to Lake Tharthar, was hit relatively harder by the droughts; reservoir storage was completely depleted by the end of 2009 for a short period. Knowledge of water availability in water-sparse regions like this is crucial for managing irrigation water use and for planning aid.

[20] In Asia, we examined the time history of storage in Toktogul Reservoir. It supplies water to Kyrgyzstan's single largest hydropower plant, and it also provides irrigation water downstream. During the 2007–2008 drought, the reservoir storage was completely depleted. Storage information for the Toktogul Reservoir is also crucial for water management in the Naryn/Syr Darya basin, which is a major international river system in Central Asia [*Siegfried and Bernauer*, 2007].

[21] With a storage capacity of 157 km^3, Lake Nasser in Africa is the third largest man-made reservoir in the world by volume. Its main use is for irrigation, with hydropower and flood control as secondary operation purposes. During the 1990s the water elevation and storage increased due to high precipitation in the Ethiopian Highlands. For the safety of the dam, water was spilled from Lake Nasser westward into the Sahara Desert, forming the Toshka Lakes

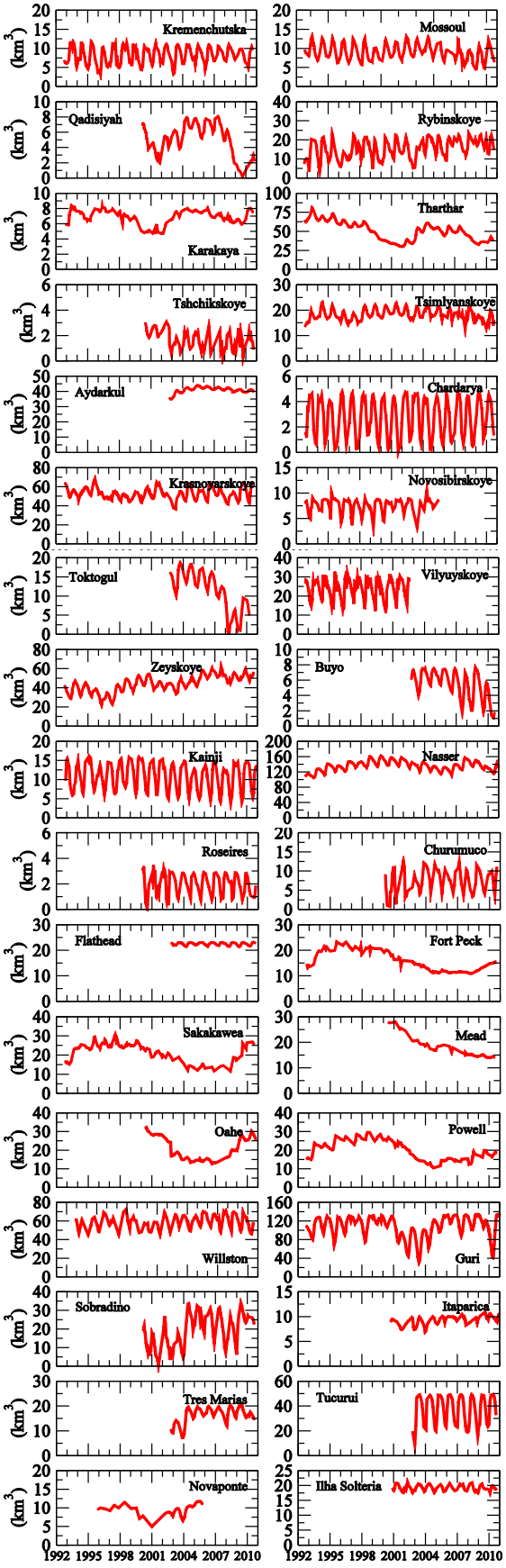

Figure 8. Global reservoir storage time series from remote sensing.

(beginning in 1998). From 2003 to 2007, these discharges to the Toshka Lakes were stopped, and the new lakes contracted [*Abdelsalam et al.*, 2008]. Our storage history for Lake Nasser shows that the rebound of storage in 2008–2009 should have allowed more spillover to the Sahara, suggesting possible increases in irrigation diversions or releases to the Nile Delta.

[22] Guri Dam in South America is the world's third largest hydropower plant. It supplies 73% of Venezuela's electricity. Two major drought events (2001 to 2004 and 2009 to 2010) were the worst in the past 40 years in Venezuela, and the reservoir dropped to a low storage of 28% of its maximum in 2003. During the 2010 event, power rationing was implemented to close the electricity gap. Our reservoir time series shows that reservoir storage experienced a quick recovery from the last drought by the end of 2010.

[23] In section 3.1, we evaluated the results for five U.S. reservoirs. Although each of these five reservoirs was affected by at least one drought during our analysis period, recovery times varied substantially as a combination of natural variation in the runoff combined with operational considerations. Among the three Missouri reservoirs, Fort Peck Reservoir (which is upstream of the other two) was the last reservoir to recover from the drought. Mostly this had to do with natural variations in runoff. From 2008 to 2010, Lake Sakakawae and Lake Oahe recovered significantly faster because a fairly large Northern Great Plains snowpack contributed to above normal runoff. However, the snowpack in the area above Fort Peck was not as big a contributing factor. With respect to the two Colorado reservoirs, Lake Powell started to recover in 2006 while Lake Mead was still deeply stressed at the end of 2010. This is because evaporation is higher in Lake Mead, which results in Lake Powell filling first during the recovery of the system.

4. Discussion

4.1. Error Sources and Description of Uncertainties

[24] Errors in estimated reservoir storage are attributable to the following: (1) altimetry water surface elevation error, (2) MODIS surface area error, (3) elevation-area relationship error, and (4) errors in the reported reservoir configurations. We examine each of these below.

4.1.1. Altimetry Water Surface Elevation Error

[25] The accuracy of the altimetry product is dominated by knowledge of the satellite orbit, the altimetric range (distance between antenna and target), the geophysical range corrections, and the target size and the tracks' location relative to the edge of the target. Satellite passes that cross over narrow reservoir extents in severe terrain will push the limits of the instruments, resulting in large errors. Major wind events, heavy precipitation, tidal effects, and the presence of ice also affect data quality and accuracy. Because each record in the reservoir's water elevation time series was calculated by averaging across the satellite ground track, this average has an associated standard error. A large standard error implies higher uncertainty for the elevation estimates. The uncertainty could be both from measurement errors and natural variations (including surface roughness and surface wind).

4.1.2. MODIS Surface Area Error

[26] Fractional water coverage for the MODIS pixels at the reservoir borders introduces error during the unsupervised classification (see section 2.2). An unrealistic seasonal

Table 2. Water Elevation-Area Relationship, Correlations, and Mean Absolute Errors

Reservoir	Dam Location (lat, lon)	Capacity (km^3)	Period of Estimated Storage	Level-Area Relationship	Correlation Coefficient	Mean Absolute Error (%)
Kremenchutska	49.08, 33.25	13.52	1992∼2010	$y = -1536.9 + 45.972x$	0.23	8
Mossoul	36.63, 42.82	12.5	1992∼2010	$y = -918.56 + 3.7919x$	0.7	5
Qadisiyah	34.21, 42.36	8.3	2000∼2010	$y = -21246 + 499.78x - 3.97x^2 + 0.0107x^3$	0.98	2
Rybinskoye	58.08, 38.75	25.4	1992∼2010	$y = 3226.3 + 13.198x$	0.09	7
Karakaya	38.23, 39.14	9.58	1992∼2010	$y = -2944 + 4.6032x$	0.78	2
Tharthar	33.79, 43.58	85.59	1992∼2010	$y = 1444.6 + 19.447x$	0.39	1
Tshchikskoye	44.99, 39.12	3.1	2000∼2010	$y = -89.297 + 13.882x$	0.7	12
Tsimlyanskoye	47.61, 42.11	23.7	1992∼2010	$y = -3914.5 + 181.39x$	0.42	8
Aydarkul	40.95, 66.5	44.3	2002∼2010	$y = -48738 + 210.28x$	0.41	1
Chardarya	41, 68	6.7	1992∼2010	$y = -8828.6 + 37.392x$	0.96	5
Krasnoyarskoye	55.5, 92	73.3	1992∼2010	$y = -5.7725 + 8.171x$	0.25	1
Novosibirskoye	54.5, 82	9.08	1992∼2004	$y = 857.13 + 2.0431x$	0.16	5
Toktogul	41.78, 72.83	19.5	2002∼2010	$y = 151.03 + 0.1471x$	0.14	2
Vilyuyskoye	62.73 111.16	35.9	1992∼2002	$y = -2121.1 + 19.197x$	0.08	5
Zeyskoye	54, 128	68.4	1992∼2010	$y = -1026.7 + 10.141x$	0.38	2
Buyo	6, −7	8.3	2002∼2010	$y = 47.495 + 2.2899x$	0.13	1
Kainji	10.4, 4.55	15	1992∼2010	$y = -4985.4 + 45.047x$	0.97	10
Nasser	23.97, 32.88	162	1992∼2010	$y = -28160 + 185.02x$	0.79	1
Roseires	11.6, 34.38	3	2000∼2010	$y = -3215.4 + 7.0832x$	0.68	9
Churumuco	18.265, −101.89	12	2000∼2010	$y = -624.09 + 6.9943x$	0.68	5
Flathead	47.67, −114.23	23.2	2002∼2010	$y = -1799 + 2.7029x$	0.32	1
Fort Peck	48, −106.42	23.05	1992∼2010	$y = -14860 + 23.19x$	0.76	3
Sakakawea	47.5, −101.42	29.38	1992∼2010	$y = -14439 + 28.339x$	0.72	3
Mead	36.01, −114.74	31.92	2000∼2010	$y = -2491 + 8.4546x$	0.83	6
Oahe	44.45, −100.39	28.54	2000∼2010	$y = -11798 + 26.661x$	0.83	13
Powell	36.94, −114.48	30	1992∼2010	$y = -8654 + 8.2567x$	0.66	2
Williston	56.01, −122.2	74	1992∼2010	$y = 1108.4 + 0.9685x$	0.11	3
Guri	7.76, −63	135	1992∼2010	$y = -354.07 + 16.948x$	0.4	2
Sobradino	−10, −42	34.1	2000∼2010	$y = -48382 + 131.55x$	0.81	4
Itaparica	−9, −39	10.8	2000∼2010	$y = -11074 + 39.052x$	0.8	1
Tres Marias	−18, −45.5	21	2002∼2010	$y = 357.44 + 0.7708x$	0.19	2
Tucurui	−3.88, −49.74	49.54	2002∼2010	$y = 1645.7 + 7.299x$	0.25	2
Novaponte	−19.15, −47.33	12.8	1995∼2005	$y = 73.749 + 0.19923x$	0.08	1
Ilha_solteira	−20, −51	21.2	2000∼2010	$y = -18518 + 59.925x$	0.59	5

variation may be introduced for the cases when the reservoir has a large shoreline to area ratio. Although the majority filter (see section 2.2) improves the classification by eliminating high-frequency noise, it tends to overestimate water area for reservoirs with a complicated shoreline and shallow mean water depth (particular when the reservoir storage is low). We use the area from the unsupervised classification (before filtering) as the minimum area, and the filtered result as the maximum area, to create a bracket for each record.

4.1.3. Water Surface Elevation-Area Relationship Error

[27] The accuracy of the elevation-area relationship depends on the quality of both variables. When one variable is systematically biased (e.g., surface area for Lake Oahe), the water surface elevation-area relationship error will be carried to the estimated storage. Although a good correlation between elevation and area generally indicates reliable storage estimation, a small correlation coefficient may also arise when the reservoir has nearly constant area (vertical walls, in which case the area does not vary much with the changing elevation). The approximation of reservoir bathymetry using a linear elevation-area relationship (except for Lake Qadisiyah) may introduce some error but in most cases does not appear to be a major contributor to the error (see section 3.1).

4.1.4. Errors in the Reported Reservoir Configurations

[28] According to equation (1), the estimated storage will be biased if the characteristics at capacity (storage, area, and elevation) are not accurate. Even when correctly documented, the storage capacity might have changed due to sedimentation over time. Nonetheless, the storage variation is free of this potential error source, since it is solely a function of remote sensing based elevation and area at different time steps (the constants at capacity will be canceled out when storage change is calculated).

[29] To represent the uncertainties, equation (1) was modified with the terms for errors represented explicitly (in equation (2)). When the storage estimation was based on surface elevation (h), A_o and ΔA_o were substituted by $f(h_o)$ and $\Delta h_o f'(h_o)$, respectively. Equation (3) shows the storage error as a function of surface level and its error. When the storage estimation was based on surface area (A), h_o and Δh_o were substituted by $f^{-1}(A_o)$ and $\Delta A_o f'(f^{-1}(A_o))$, respectively. Equation (4) shows the storage error as a function of surface area and its error.

$$V_o + \Delta V_o = V_c - (A_c + A_o + \Delta A_o)(h_c - h_o - \Delta h_o)/2 \quad (2)$$

$$\Delta V_o = \Delta h_o(A_c + f(h_o))/2 + h_o f(h_o)/2 - \Delta h_o f'(h_o)(h_c - h_o)/2 + (\Delta h_o)^2 f'(h_o)/2 \quad (3)$$

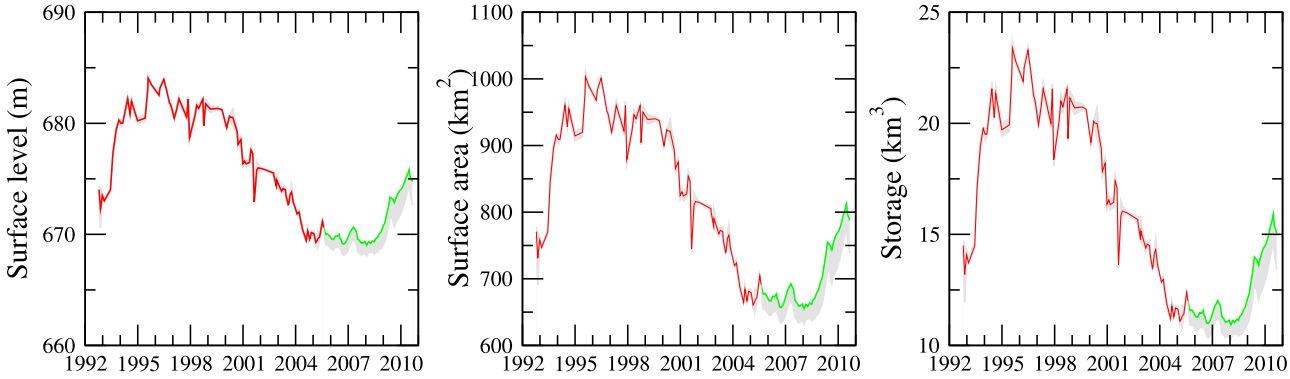

Figure 9. Ranges of surface level, area, and storage estimates at Fort Peck Reservoir, with the ranges represented by shaded area in gray, altimetry-based estimates in red, and MODIS-based estimates in green.

$$\Delta V_o = \Delta A_o f'\left(f^{-1}(A_o)\right)(A_c + A_o))/2 + A_o f^{-1}(A_o)/2 - \Delta A_o\left(h_c - f^{-1}(A_o)\right)/2 + (\Delta A_o)^2 f'\left(f^{-1}(A_o)\right)/2 \quad (4)$$

[30] As described above, errors were provided for the elevation, area, and storage at each reservoir. Figure 9 shows the results for Fort Peck Reservoir as an example. For the period when water elevation was inferred from surface area, its error was estimated by $\Delta A_o f'(f^{-1}(A_o))$. Likewise, when area was inferred from elevation, its error was calculated by $\Delta h_o f'(h_o)$. For Fort Peck Reservoir, the mean absolute errors (over the entire period) of elevation, area, and storage are 0.87 m, 20.24 km^2, and 0.65 km^3, respectively. The mean absolute errors of storage as a percentage of reservoir capacity were plotted against the capacity in Figure 10 (data are given in Table 2). Figure 10 suggests that as the capacity increases, the uncertainty of the estimation decreases. For all of the reservoirs larger than 40 km^3, the mean absolute errors are less than 3%. The reservoir with the worst performance is Lake Oahe (13.0%), which results from overestimation of the area (from large shoreline to sqrt(area) ratio)). The errors are consistent with the validation results in section 3.1. For the two smallest reservoirs (Tshchikskoye and Roseires), the mean absolute errors are 11.6% and 9.3%. As the size of the reservoir decreases, there is a greater chance that the altimeters will have short overpasses (fewer elevation samples) and the modest resolution of MODIS will affect area estimations. The average value for the errors in Figure 10 is 4%.

4.2. Future Opportunities

[31] A key constraint on remotely sensed reservoir storage is the limited number of altimetry-based reservoir surface elevation products. Due to their narrow swaths, large footprints, and effects of surrounding topography, current generation spaceborne radar altimeters can only monitor water elevations for a relatively small number of large reservoirs. Furthermore, the accuracy of the MODIS estimates of surface area is limited by modest resolution (250 m). The future Surface Water Ocean Topography (SWOT) mission [*Biancamaria et al.*, 2010; *Durand et al.*, 2010; *Lee et al.*, 2010] in contrast will be revolutionary for understanding global inland total fresh water storage. As contrasted with current generation nadir-looking altimeters, SWOT will be a wide-swath instrument which will provide images, rather than tracks. It is expected to achieve spatial resolution on the order of tens of meters (for purposes of identifying water surfaces, as contrasted with 250 m for MODIS) and centimetric vertical precision when averaged over targets of interest (i.e., one or more km^2 of surface area). However, SWOT launch is not expected until 2020; hence the methods developed here should prove useful for studying selected large representative reservoirs for the next decade.

5. Conclusions

[32] We generated a global reservoir storage data set based (aside from ancillary information about reservoirs at capacity) solely from satellite remote sensing (with surface elevation and area by-products). To this end, we first developed an algorithm to estimate surface area time series for selected large reservoirs (primarily based on the availability of altimetry water elevation products) from MODIS 16-day 250 m vegetation index images. The water elevation (from altimetry products) and surface area (from MODIS) were used to derive the elevation-area relationships for each reservoir, such that either the water elevation or surface area can be inferred from its counterpart when direct observation is unavailable. Together, time histories for 34 global reservoirs were derived and the results were evaluated using

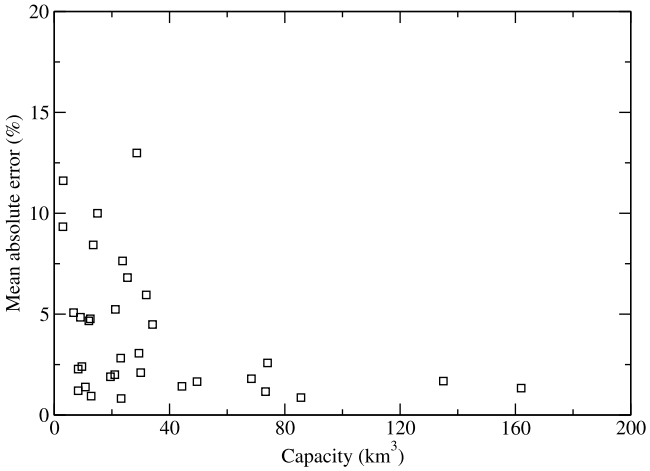

Figure 10. The mean absolute error as a percentage of reservoir capacity.

observational data at five of these reservoirs (each located in the U.S.). Our overall conclusions are as follows:

[33] 1. The MODIS-based water classification approach generally works for these large reservoirs. In spite of its relatively coarse spatial resolution, the daily coverage of MODIS is a manifest advantage over the low repeat frequency satellite sensors (e.g., Landsat, SARs). In addition, the use of the unsupervised K-means clustering approach (as contrasted with empirical thresholds) promotes consistencies among the classified water area for the globally distributed reservoirs.

[34] 2. The storage estimates were highly correlated with observations (0.92 to 0.99), with relatively small NRMSE values (3% to 15%). Although a low correlation between the derived surface elevation and area can result from many conditions, a high correlation usually indicates good quality for both data sets. The method works best for reservoirs where the shoreline-to-area ratios are small. Where this is not the case, overestimations of surface area are likely to occur. When the reservoir has long shorelines surrounded by seasonal vegetation, the MODIS-estimated storage tends to have an exacerbated seasonality which does not agree with the altimetry-base estimates. A moving average can be used to filter this false signal.

[35] 3. Both the remotely sensed water elevation and surface area had errors, usually resulting from a combination of each sensor's limitations and the retrieval algorithms. Such errors were propagated into the storage estimates. An error model was constructed that assessed the uncertainty of storage as a function of surface level and its error for altimetry-based estimates (or a function of area and its error for MODIS-based estimations). Mean absolute errors range from 1% to 13% (as a percentage of capacity), with the error decreases as the reservoir capacity increases. Of the 34 reservoirs, 31 have mean absolute errors less than 10%.

[36] 4. Due to the limitations of current generation satellite radar altimeters and the relatively coarse spatial resolution of MODIS, only a small number of large reservoirs were studied here. Until the SWOT instrument is available in 2020, methods developed here should prove useful for providing multidecade records over selected large representative reservoirs.

[37] **Acknowledgments.** The altimetry products used in this study were downloaded from the U.S. Department of Agriculture's (USDA) Global Reservoir and Lake Elevation Database (http://www.pecad.fas.usda.gov/cropexplorer/global_reservoir/) and French Space Agency's (CNES) Hydrology by Altimetry (http://www.legos.obs-mip.fr/soa/hydrologie/hydroweb). Bryan W. Wuerker and. Richard B. Clayton of the U.S. Bureau of Recreation provided reservoir observations for Lakes Mead and Powell. Observations for Lakes Peck, Oahe, and Sakakawea were provided by the U.S. Army Corps of Engineers (http://www.nwd-mr.usace.army.mil/rcc/projdata/projdata.html). We also thank Sylvain Biancamaria for advice on water classification methods and Michael A. Swenson for explain the recovery of the Missouri reservoirs. The work reported herein was supported by NASA grant No. NNX08AN40A under its Making Earth System data records for Use in Research Environments program, and by grant No. NNX08AM72G under the Applied Sciences/Decision Support program.

References

Abdelsalam, M. G., et al. (2008), Rise and demise of the New Lakes of Sahara, *Geosphere*, *4*(2), 375–386, doi:10.1130/GES00142.1.

Aladin, N., J. F. Crétaux, I. S. Plotnikov, A. V. Kouraev, A. O. Smurov, A. Cazenave, A. N. Egorov, and F. Papa (2005), Modern hydro-biological state of the Small Aral sea, *Environmetrics*, *16*(4), 375–392, doi:10.1002/env.709.

Alsdorf, D., et al. (2001), Water level changes in a large Amazon lake measured with spaceborne radar interferometry and altimetry, *Geophys. Res. Lett.*, *28*(14), 2671–2674, doi:10.1029/2001GL012962.

Alsdorf, D. E., et al. (2007), Measuring surface water from space, *Rev. Geophys.*, *45*, RG2002, doi:10.1029/2006RG000197.

Anderberg, M. R. (1973), *Cluster Analysis for Applications*, Academic, San Diego, Calif.

Berry, P. A. M., et al. (2005), Global inland water monitoring from multimission altimetry, *Geophys. Res. Lett.*, *32*, L16401, doi:10.1029/2005GL022814.

Biancamaria, S., et al. (2010), Preliminary characterization of SWOT hydrology error budget and global capabilities, *IEEE J. of Selected Topics in Appl. Earth Obs. and Remote Sens.*, *3*(1), 6–19, doi:10.1109/JSTARS.2009.2034614.

Biemans, H., et al. (2011), Impact of reservoirs on river discharge and irrigation water supply during the 20th century, *Water Resour. Res.*, *47*, W03509, doi:10.1029/2009WR008929.

Birkett, C. (1994), Radar altimetry - A new concept in monitoring global lake level changes, *Eos Trans. AGU*, *75*(24), 273–275, doi:10.1029/94EO00944.

Birkett, C. M. (1995), The contribution of TOPEX/POSEIDON to the global monitoring of climatically sensitive lakes, *J. Geophys. Res.*, *100*(C12), 25,179–25,204, doi:10.1029/95JC02125.

Birkett, C. M. (2000), Synergistic remote sensing of Lake Chad: Variability of basin inundation, *Remote Sens. Environ.*, *72*(2), 218–236, doi:10.1016/S0034-4257(99)00105-4.

Birkett, C. M., and B. Beckley (2010), Investigating the Performance of the Jason-2/OSTM Radar Altimeter over Lakes and Reservoirs, *Marine Geodesy*, *33*, 204–238, doi: 10.1080/01490419.2010.488983.

Bobrowski, L., and J. C. Bezdek (1991), C-means clustering with the L1 and L–infinity norms, *IEEE Trans. Syst. Man Cybern.*, *21*(3), 545–554, doi:10.1109/21.97475.

Carroll, M. L., et al. (2009), A new global raster water mask at 250 m resolution, *Int. J. of Digital Earth*, *2*(4), 291–308, doi:10.1080/17538940902951401.

Chao, B. F., et al. (2008), Impact of artificial reservoir water impoundment on global sea level, *Science*, *320*(5873), 212–214, doi:10.1126/science.1154580.

Chelton, D. B., E. J. Walsh, and J. L. MacArthur (1988), "Nuts and bolts" of satellite radar altimetry, in *Proceedings of the NASA/WOCE Altimeter Algorithm Workshop*, *U. S. WOCE Tech. Rep. 2*, edited by D. B. Chelton, pp. 1-43, NASA, Corvallis, Ore.

Crétaux, J. F., et al. (2005), Evolution of sea level of the big Aral Sea from satellite altimetry and its implications for water balance, *J. Great Lakes Res.*, *31*(4), 520–534, doi:10.1016/S0380-1330(05)70281-1.

Crétaux, J. F., et al. (2011), SOLS: A lake database to monitor in the Near Real Time water level and storage variations from remote sensing data, *Adv. Space Res.*, *47*(9), 1497–1507, doi:10.1016/j.asr.2011.01.004.

Döll, P., and S. Siebert (2002), Global modeling of irrigation water requirements, *Water Resour. Res.*, *38*(4), 1037, doi:10.1029/2001WR000355.

Döll, P., et al. (2009), Global-scale analysis of river flow alterations due to water withdrawals and reservoirs, *Hydrol. Earth Syst. Sci.*, *13*(12), 2413–2432, doi:10.5194/hess-13-2413-2009.

Durand, M., et al. (2010), The surface water and ocean topography mission: Observing terrestrial surface water and oceanic submesoscale eddies, *Proc. IEEE*, *98*(5), 766–779, doi:10.1109/JPROC.2010.2043031.

Haddeland, I., et al. (2006), Anthropogenic impacts on continental surface water fluxes, *Geophys. Res. Lett.*, *33*, L08406, doi:10.1029/2006GL026047.

Hanasaki, N., et al. (2006), A reservoir operation scheme for global river routing models, *J. Hydrol.*, *327*(1–2), 22–41, doi:10.1016/j.jhydrol.2005.11.011.

International Commission on Large Dams (2007), *World Register of Dams*, Paris.

Islam, A. S., et al. (2010), Flood inundation map of Bangladesh using MODIS time-series images, *J. Flood Risk Manage.*, *3*(3), 210–222, doi:10.1111/j.1753-318X.2010.01074.x.

Lee, H., et al. (2010), Characterization of surface water storage changes in Arctic lakes using simulated SWOT measurements, *Int. J. Remote Sens.*, *31*(14), 3931–3953, doi:10.1080/01431161.2010.483494.

Lehner, B., and P. Döll (2004), Development and validation of a global database of lakes, reservoirs and wetlands, *J. Hydrol.*, *296*(1–4), 1–22, doi:10.1016/j.jhydrol.2004.03.028.

Lehner, B., et al. (2011), High-resolution mapping of the world's reservoirs and dams for sustainable river-flow management, *Front. Ecol. Environ*, *9*(9), 494–502, doi:10.1890/100125.

Lettenmaier, D. P., and P. C. D. Milly (2009), Land waters and sea level, *Nat. Geosci.*, *2*(7), 452–454, doi:10.1038/ngeo567.

MacQueen, J. B. (1967), Some methods for classification and analysis of multivariate observations, paper presented at the 5th Berkeley Symposium on Mathematical Statistics and Probability, Univ. of Calif. Press, Berkeley, Calif.

McKellip, R. B. B., et al. (2004), *PECAD's Global Reservoir and Lake Monitor: A Systems Engineering Report, Version 1.0*, NASA John C. Stennis Space Cent., Miss.

Mercier, F., et al. (2002), Interannual lake level fluctuations (1993–1999) in Africa from Topex/Poseidon: Connections with ocean-atmosphere interactions over the Indian Ocean, *Global Planet. Change*, *32*(2–3), 141–163, doi:10.1016/S0921-8181(01)00139-4.

Nilsson, C., et al. (2005), Fragmentation and flow regulation of the world's large river systems, *Science*, *308*(5720), 405–408, doi:10.1126/science.1107887.

Ordoyne, C., and M. A. Friedl (2008), Using MODIS data to characterize seasonal inundation patterns in the Florida Everglades, *Remote Sens. Environ.*, *112*(11), 4107–4119, doi:10.1016/j.rse.2007.08.027.

Ross, K. M. R. (2006), *Verification and Validation of NASA-Supported Enhancements to PECAD's Decision Support Tools*, NASA John C. Stennis Space Cent., Miss.

Rost, S., et al. (2008), Agricultural green and blue water consumption and its influence on the global water system, *Water Resour. Res.*, *44*, W09405, doi:10.1029/2007WR006331.

Sawunyama, T., et al. (2006), Estimation of small reservoir storage capacities in Limpopo River Basin using geographical information systems (GIS) and remotely sensed surface areas: Case of Mzingwane catchment, *Phys. Chem. Earth*, *31*(15–16), 935–943.

Selim, S. Z., and M. A. Ismail (1984), K-means-type algorithms - A generalized convergence theorem and characterization of local optimality, *IEEE Trans. Pattern Anal. Mach. Intell.*, *6*(1), 81–87, doi:10.1109/TPAMI.1984.4767478.

Siegfried, T., and T. Bernauer (2007), Estimating the performance of international regulatory regimes: Methodology and empirical application to international water management in the Naryn/Syr Darya basin, *Water Resour. Res.*, *43*, W11406, doi:10.1029/2006WR005738.

Smith, L. C., and D. E. Alsdorf (1998), Control on sediment and organic carbon delivery to the Arctic Ocean revealed with spaceborne synthetic aperture radar: Ob' River, Siberia, *Geology*, *26*(5), 395–398, doi:10.1130/0091-7613(1998)026<0395:COSAOC>2.3.CO;2.

Tang, Q. H., et al. (2009), Remote sensing: Hydrology, *Prog. Phys. Geogr.*, *33*(4), 490–509, doi:10.1177/0309133309346650.

Trigo, R. M., C. Gouveia, and D. Barriopedro (2010), The intense 2007–2009 drought in the Fertile Crescent: Impacts and associated atmospheric circulation, paper presented at General Assembly, Eur. Geophys. Union, Vienna.

Vörösmarty, C. J., C. Lévêque, and C. Revenga (2005), Fresh water, in *Millennium Ecosystem Assessment: Ecosystems and Human Well-Being: Current State and Trends*, edited by R. S. R. Hassan and N. Ash, pp. 166–207, Island Press, Washington, D. C.

Wang, Y., et al. (2008), Using MODIS images to examine the surface extents and variations derived from the DEM and laser altimeter data in the Danjiangkou Reservoir, China, *Int. J. Remote Sens.*, *29*(1), 293–311, doi:10.1080/01431160701253311.

Wisser, D., et al. (2008), Global irrigation water demand: Variability and uncertainties arising from agricultural and climate data sets, *Geophys. Res. Lett.*, *35*, L24408, doi:10.1029/2008GL035296.

Xiao, X. M., et al. (2006), Mapping paddy rice agriculture in South and Southeast Asia using multi-temporal MODIS images, *Remote Sens. Environ.*, *100*(1), 95–113, doi:10.1016/j.rse.2005.10.004.

Xu, K. Q., et al. (2006), Measuring water storage fluctuations in Lake Dongting, China, by Topex/Poseidon satellite altimetry, *Environ. Monit. Assess.*, *115*(1–3), 23–37.

Yan, Y. E., et al. (2010), Detecting the spatiotemporal changes of tidal flood in the estuarine wetland by using MODIS time series data, *J. Hydrol.*, *384*(1–2), 156–163, doi:10.1016/j.jhydrol.2010.01.019.